LBL-20686
Preprint c.2

Lawrence Berkeley Laboratory
UNIVERSITY OF CALIFORNIA

Accelerator & Fusion Research Division

RECEIVED
LAWRENCE
BERKELEY LABORATORY

AUG 13 1986

LIBRARY AND
DOCUMENTS SECTION

Submitted to Nuclear Fusion

HELICALLY LINKED MIRROR CONFIGURATION

P. Ranjan and W.B. Kunkel

December 1985

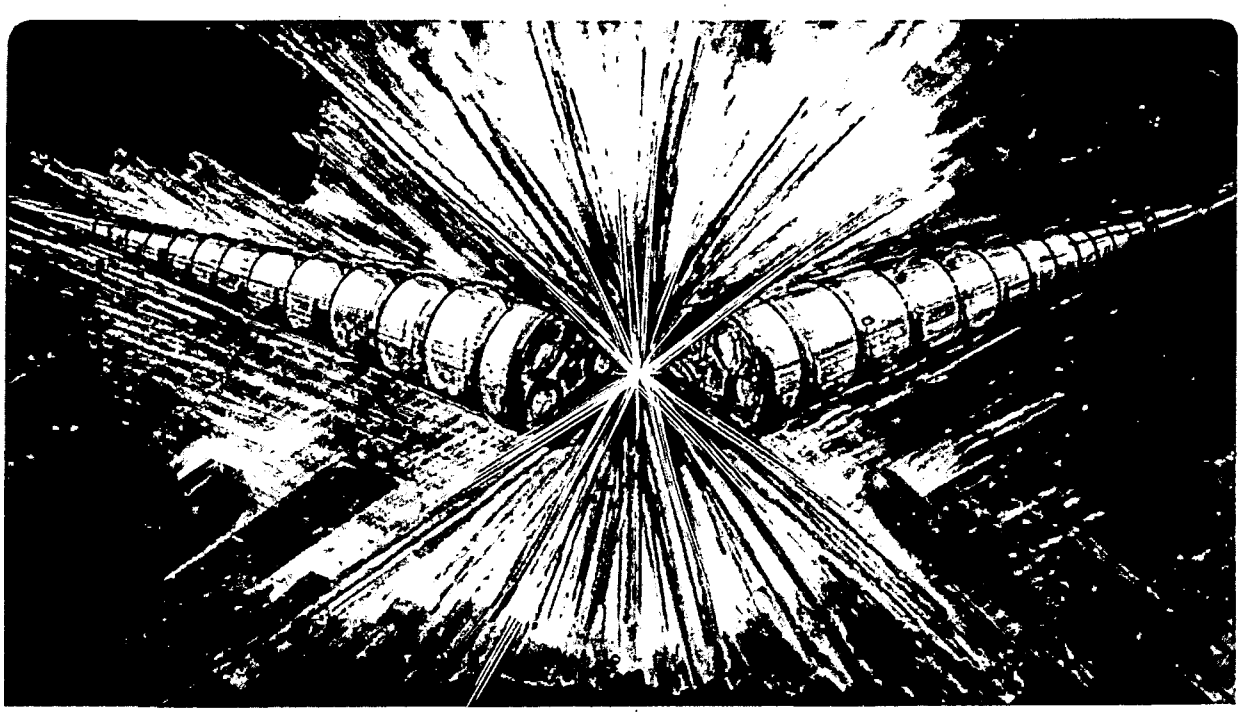

LBL-20686 c.2

Prepared for the U.S. Department of Energy under Contract DE-AC03-76SF00098

DISCLAIMER

This document was prepared as an account of work sponsored by the United States Government. While this document is believed to contain correct information, neither the United States Government nor any agency thereof, nor the Regents of the University of California, nor any of their employees, makes any warranty, express or implied, or assumes any legal responsibility for the accuracy, completeness, or usefulness of any information, apparatus, product, or process disclosed, or represents that its use would not infringe privately owned rights. Reference herein to any specific commercial product, process, or service by its trade name, trademark, manufacturer, or otherwise, does not necessarily constitute or imply its endorsement, recommendation, or favoring by the United States Government or any agency thereof, or the Regents of the University of California. The views and opinions of authors expressed herein do not necessarily state or reflect those of the United States Government or any agency thereof or the Regents of the University of California.

LBL-20686

Helically Linked Mirror Configuration*

P. Ranjan and W. B. Kunkel

Lawrence Berkeley Laboratory

University of California

Berkeley, CA 94720

December 1985

Abstract

The scheme of helical linking of magnetic mirror sections to eliminate longitudinal loss of particles due to the velocity space loss-cone is described. An approximate theoretical treatment of the scheme is given along with numerical evaluations of vacuum magnetic field properties and of single particle motion. An estimate of the maximum equilibrium beta due to the limitation on transverse displacement of the plasma boundary is also given. Good elimination of longitudinal loss and reasonably high beta value make the scheme an attractive one, to be pursued further.

* This work was supported by U.S. DOE under Contract No. DE-AC03-76SF00098.

I. Introduction

Efforts to reduce end losses in mirror-confined plasmas by means of ambipolar potential barriers has led to ever increasing complexity of the so-called tandem-mirrors [1]. We have therefore decided to take a new look at the possibility of linking up a set of mirror cells into a closed arrangement. This is topologically similar to configurations proposed before, some of which have been abandoned [2] while others are still under study [3,4]. Our scheme differs from all of these by the incorporation of a rotational transform. In the arrangement discussed here, the transform is produced by making the links between mirrors out of solenoids bent into helical sections (see Fig. 1). In a sense, this configuration can therefore also be thought of as a type of stellarator or Heliac, the volume of which is greatly enlarged by insertion of straight axisymmetric mirror sections. The latter can presumably operate at relatively high values of beta, consistent with the reduced field between mirrors, leading to an enhanced average beta. Other advantages and disadvantages of this system in comparison with conventional toroidal confinement schemes need to be discussed, of course. In this paper we are looking only at two parts of the problem, i.e., at single-particle confinement properties of this arrangement using simple helical bends made of circular coils and at the beta-limit set by the radial displacement of the plasma column in the helical sections. The concept was first described in 1982 [5].

The configuration has very high rotational transform and thus single particle confinement of passing particles is good. We think it is possible to use noncircular magnetic surfaces to achieve an average magnetic well and also have vanishingly small charge-neutralization current flowing through the straight section. However, work done in this direction will be published in a later paper.

II. Description of geometry

The device has to be nonplanar to make use of helical linking in a smooth way. The geometric axis of the device consists of alternating straight and helical segments. For the device to have n-straight segments we generate the helical axis by wrapping the straight line over a cylinder, whose axis is at an angle π/n to the straight line. This makes the transition smooth up to first order. However, the curvature and the torsion are discontinuous at the transition point. The angle by which the straight line wraps around the cylinder is dependent upon the length of the straight segment desired and the radius of the generating cylinder. The torsion, and hence, the rotational transform is determined from these parameters. The details of the construction and program used to create the coil data will be given in a separate future LBL-report.

The selection of the number of segments is dependent upon various considerations. A full study of this and optimization of parameters for a reactor type device or otherwise has not been undertaken as yet. However, as shown in Fig. 1, the number of segments we have chosen to study is the lowest possible, i.e. n=3. (The n=2 case is simply a racetrack configuration, which does not have any torsion and thus no rotational transform.) We call the device THELMA (an acronym for Triangular Helically Linked Mirror Arrangement).

The spacing of the coils to generate the desired field can be chosen in a way to have the smallest possible ripple on the magnetic axis (say, less than 1%). In the helical sections the magnetic field does not vary very much along the helix but is of course a function of distance along the local radius of curvature. Particles with small velocity ratio $v_{\parallel}/v_{\perp}$ there will experience relatively large drift excursions that depend on their position. Thus if the strongest fields in the system are within the bends the trajectories of barely

passing and of reflected particles in these regions will not be axisymmetric and will give rise to neoclassical drift-orbit diffusion of the class of particles that enter the helical sections with very small parallel velocities. We decided to minimize this effect in the present system by the addition of strong axisymmetric mirror "throats" (or "bottlenecks") at the ends of each of the straight sections. The magnetic fields in the mirror throats (B_t) of the axisymmetric straight sections must all be equal to each other and must be stronger than anywhere else on any given flux surface (see Fig. 2). In this way any particle within the loss-cone of any mirror section will pass through all mirrors until it is scattered into a trapped orbit. If a particle is trapped in a straight section it will carry out only axisymmetric drift motions and hence its diffusion will not be subject to neoclassical effects until it is detrapped and becomes a passing particle again. Only particles trapped in the helical bends will perform banana orbits and hence contribute to neoclassical diffusion, or worse, i.e., will drift out rapidly in a few bounces. Presumably, the number of particles so affected could be limited to a very small fraction of the total number in the device. These considerations were presented by Abt and Kunkel in 1983 [6], but a thorough quantitative analysis has not yet been carried out.

The criterion for passing particles given above relates the minimum mirror ratio for the helical sections to their aspect ratio. Somewhat stronger mirror peak fields (B_t) are desirable to give the marginally passing particles a reasonable pitch angle throughout the helical region. This is indicated in Fig. 2. The mirror ratio, R, in the axisymmetric straight sections, on the other hand, should be made much larger to maximize the benefit from the difference between the two regions. This can be expressed formally by

the relation

$$R \gg \sqrt{(1+2\kappa r)}$$

where κ denotes the curvature and r is the maximum transverse dimension in the helical section. The relation between various magnetic fields can be expressed as (shown in Fig. 2)

$$B_t > B_h > B_s$$

III. Analytical treatment

If we do not take into consideration the discontinuity in curvature and torsion at the junction of straight and helical sections, then, we can get a good approximation for the vacuum magnetic field inside the device by treating it as a solenoid with continuous and well behaved curvature and torsion. In that case, following ref. [7], we can use the Mercier coordinate system to calculate the magnetic field. Thus we define a Mercier coordinate system (ρ, ω, s), where s is the arc-length along the axis, ρ is the radial distance and ω is defined by

$$\omega = \theta + \int \chi ds \tag{1}$$

where χ denotes the torsion and θ is the angle from the principal normal. In this system we have the square of element of length

$$dl^2 = d\rho^2 + \rho^2 d\omega^2 + (1 - \kappa\rho \cos\theta)^2 ds^2 \tag{2}$$

Laplace's equation for the scalar potential ϕ associated with the magnetic field takes the form

$$\nabla^2\phi = \frac{1}{\rho}\frac{\partial}{\partial\rho}[(1 - \kappa\rho\cos\theta)\frac{\rho\partial\phi}{\partial\rho}] + \frac{1}{\rho^2}\frac{\partial}{\partial\omega}[(1 - \kappa\rho\cos\theta)\frac{\partial\phi}{\partial\omega}]$$

$$+ \frac{\partial}{\partial s}[\frac{1}{1 - \kappa\rho\cos\theta}\frac{\partial\phi}{\partial s}] = 0 \tag{3}$$

Now we expand the Laplace equation in $\kappa\rho$ as $\kappa\rho \ll 1$

Then if we assume that in the zeroeth order $\underline{B} = B_0 \hat{e}_s$ i.e. the magnetic field is axial, we obtain the scalar potential as

$$\phi = B_0 s + \frac{B_0}{8} (3a^2 - \rho^2) \frac{\partial}{\partial s} (\kappa\rho \cos \theta) \tag{4}$$

where a is the radius of the ideally conducting solenoid. Any magnetic surface defined by ψ = const satisfies $\underline{B} \cdot \nabla\psi = 0$ and is found in this case to be given by

$$\psi = \rho^2 - \frac{3}{4} (a^2 - \rho^2) \kappa\rho \cos \theta = \text{const.} \tag{5}$$

The displacement of the magnetic axis from the geometric axis is $\Delta\rho = \frac{3}{8} \kappa a^2$ in the direction of the principal normal.

If we look at the terms carefully, we expect the magnetic surfaces to have circular cross sections in the middle of the helical section. However, the center of the circles are displaced with respect to the geometric center and the amount of displacement decreases as we go away from the center. Thus it may look somewhat as shown in Fig. 3. In the middle of the straight section we would expect concentric circular magnetic surfaces, which may change due to the discontinuous transition region. However one only expects a qualitative agreement with this approximate model, which may be sufficient to understand the various numerical calculation outputs.

Now let us consider the drift orbits of single particles in this type of magnetic field configuration on the basis of this model following ref. [8]. The guiding center velocity including the curvature and grad-B drift is given by

$$\frac{d\vec{r}}{dt} = V_{\parallel}\frac{\vec{B}}{B} + \frac{mc}{2eB^3}(2V_{\parallel}^2 + V_{\perp}^2)(\vec{B} \times \nabla B) \tag{6}$$

$$= \frac{V_{\parallel}}{B}[\vec{B} + r_g(V_{av})(\hat{B} \times \nabla B)], \qquad \text{where} \begin{cases} r_g(V_{av}) = \dfrac{mc\ V_{av}}{eB} \\ V_{av} = V_{\parallel} + \dfrac{V_{\perp}^2}{2V_{\parallel}} \end{cases}$$

$$V_{\perp}^2 / B = \text{Const.}$$

$$V_{\perp}^2 + V_{\parallel}^2 = V_o^2 = \text{Const.} \tag{7}$$

In guiding center approximation the drift orbit surfaces, in such a system with magnetic surfaces, form modified or "pseudo-magnetic surfaces" with effective magnetic field given by

$$\vec{B}^* = \vec{B} + r_g(V_{av})(\hat{B} \times \nabla B) = \vec{B} + \vec{B}_1 \tag{8}$$

This can be shown to be consistent with the drift equation (6) by expressing the latter in the form

$$\frac{d\vec{r}}{dt} = \frac{V_{\parallel}}{B}\vec{B}^* \simeq V_{\parallel}\frac{\vec{B}^*}{|\vec{B}^*|} \qquad \text{as } |\vec{B}_1| << |\vec{B}| \tag{9}$$

In terms of velocity ratio we express the effective magnetic field, whose field lines represent the drift orbits of particle guiding centers, as

$$\vec{B}^* = \vec{B} + \frac{mcV_o}{eB^2}\frac{(1 + 1/2\gamma_v^2)(\vec{B} \times \nabla B)}{\sqrt{1 + 1/\gamma_v^2}} \simeq \vec{B} + \frac{mcV_o}{eB^2}(1 + 1/8\gamma_v^4)(\vec{B} \times \nabla B) \tag{10}$$

$$(\text{for } \gamma_v \equiv v_{\parallel}/v_{\perp} \geq 1.4)$$

From this we note that the perturbation term and hence the drift orbit deviation from the magnetic field lines-

(a) depends on sign of charge

(b) is insensitive to velocity ratio γ_v for $\gamma_v > 1.0$

(c) is proportional to the square root of the particle energy.

By treating the perturbation term B_1 as small one can show [11] that the deviation Δ of the drift orbit surfaces from the magnetic surfaces is roughly given by

$\Delta \sim r_g(v_{av}) \cdot \frac{\kappa L}{\iota}$, where L denotes the total length of the system and iota (ι) is the rotational transform, as usual.

Thus for $\frac{\kappa L}{\iota} \sim 1$, $\Delta \sim r_g(V_{av})$, hence the deviation is very small for particles having small gyroradius. Thus if the field lines are confined, the drift orbits of the particles in the single-particle approximation are expected to be confined.

The expected rotational transform of the field lines on the basis of this model is simply the transform provided by the torsion of the helical sections. Thus on the axis

$$\iota = \oint \chi ds$$

Since torsion, $\chi = (\lambda/2\pi)/[(d/2)^2 + (\lambda/2\pi)^2]$ = const. for a straight helix, where λ is the pitch length, d the diameter of generating cylinder. In our case $\lambda = \pi d/2$ and each helical section has 2/3 period, so that we get the total rotational transform as

$$\iota = (3)(\tfrac{2}{3}) \frac{2\pi\lambda}{\sqrt{\lambda^2 + 4\pi^2(d/2)^2}} = \frac{4\pi}{\sqrt{5}} \simeq 322^0 \qquad (11)$$

We expect only a small amount of shear to be present in the device with plane circular coils, since in this approximation the transform does not depend on ρ.

IV. Numerical study of vacuum magnetic field property

For the vacuum magnetic field calculation the "HELIAC" [9] code was used. However the code was modified to take into account the fact that the device under consideration has three-dimensional geometry. Some other changes including replacement of magnetic field calculation subroutines were incorporated.

Here we show some vacuum magnetic field properties using the above-mentioned code. The spacing of the coil chosen was such that the magnetic field ripple was less than 1% on the magnetic axis (as shown in Fig. 4a). The three-fold symmetry, as is to be expected from design of the device, is reflected in the variation of the magnetic field on the magnetic axis with azimuthal angle. Slight asymmetry is due to the approximation in locating the magnetic axis. Zero of the azimuthal angle represents the middle of a helical section. Figure 4b shows the variation of magnetic field magnitude B on the magnetic axis when a mirror field is introduced in the straight section, by changing the current in the coil.

Figure 5a and 5b show the puncture plot of the field lines in the middle of straight and helical sections respectively. As is clear from the figures the field lines seem to form well-defined nested magnetic surfaces. Different symbols represent different starting points for the field lines. If one looks carefully, the outermost magnetic surface starts showing some oscillatory nature and breaks apart as we go further away from the magnetic axis. The radial distance at which this occurrs is sensitive to the ripples in the magnetic field. Less ripple increases the area in which field lines form closed magnetic surfaces. This has a direct effect on the behavior of single particle motion, as expected theoretically.

The variation of rotational transform with radial distance seems to first increase and then decrease as we go away from the magnetic axis as shown in Fig. 6, however the net variation in rotational transform is very small. Thus shear is also small. The agreement with the approximate calculation of the rotational transform on axis is good. Also one should note that the rotational transform is not passing through any region of low-number rational multiple of 2π.

V. Single particle motion

To study the drift orbit motion of single particles in the given magnetic field configuration the "TIBRO-X" [10] code was used. However the magnetic field calculation was vectorized and a different output package was developed. To compare with the approximate theoretical model we show here a typical output for the simplified case when there are no mirrors in the straight section (R=1), and

radius of coil, a=0.125 m

total arc-length=9.6 m

curvature, κ = 2.2 m^{-1}

torsion, χ = 1.1 m^{-1}

energy, E =0.2 KeV

magnetic field = 0.3 T (in the middle of the straight section)

$V_{\parallel}/V_{\perp} = 2.0$

Figure 7 shows the variation of the radial distance of the guiding center from the geometrical axis with respect to the distance along the axis. The radial distance remains constant in the straight section but changes in the helical section. Poincare plots in the middle of the helical section show

that the drift orbits lie on closed curves, hence the orbits are confined. The center of the orbits is displaced with respect to the geometrical center. Figure 8a shows the variation of drift orbit surface Poincare plots in the middle of helical section with radial distance. The drift orbits do not remain closed beyond a certain maximum radial distance. The regions of closed orbits and open orbits overlap a little bit at the boundary. Whether an orbit is closed or open in this transition region depends on the pitch angle. Figures 8b and 8c show the dependence on sign of charge and pitch angle. These are in qualitative agreement with the theoretical model.

VI. Estimate of equilibrium beta value

One can make an estimate of the maximum equilibrium beta by considering the displacement of magnetic surfaces in the presence of plasma due to the curvature of the system. The transverse displacement of the magnetic surfaces which is dependent on the beta value of the plasma is limited by the transverse dimension of the device under consideration.

For this we follow ref. [8]. Physically the procedure corresponds to calculating the displacement of magnetic surfaces as a cylindrically symmetric plasma column is bent into the shape under consideration. We make the assumption of small curvature and assume that the cross-section of the magnetic surfaces is circular. Both these assumption are justified for the device we have under consideration.

Again using the Mercier coordinate system as defined earlier the magnetic surfaces may be represented as

$$\rho = \rho_0 + \xi(\rho_0,\omega,s) = \rho_0 + \mathrm{Re} \sum_n \xi_n(\rho_0) e^{i(\omega - \chi_n s)} \tag{12}$$

with

$$x_n = \frac{1}{L} \int_0^L x ds - \frac{2\pi n}{L} \tag{13}$$

Linearizing the usual plasma equilibrium equations in $\kappa\rho$, for the case in which there is no longitudinal current in the zeroeth approximation, we obtain the equation for the nth Fourier component of the displacement, ξ_n, as

$$\frac{1}{\rho}\frac{d}{d\rho}\left[\frac{\rho(x_n\rho\, B_{so})^2}{1 + x_n^2\,\rho^2} \cdot \frac{d\xi_n}{d\rho}\right]$$

$$- \frac{x_n^2\,\xi_n - \kappa_n}{1 + x_n^2\,\rho^2}\left[\frac{2\, x_n^2\,\rho^2\, B_{so}^2}{1 + x_n^2\,\rho^2} + (x_n\,\rho\, B_{so})^2 + 8\pi\rho\,\frac{dp_o}{d\rho}\right] = 0 \tag{14}$$

For the case when $|x_n\rho| << 1$ i.e. when we can terminate the approximation for low values of n, we get (In our case we can terminate the Fourier series at n=7, without appreciable error. For this the approximation is justified).

$$\xi_n = -\frac{3}{8}\,\kappa_n\rho^2\left(1 - \frac{b^2}{\rho^2}\right) + \frac{\kappa_n\beta}{2x_n^2}\left(1 - \frac{b^2}{\rho^2}\right) \text{ for } \rho \geq b \tag{15}$$

where b is the plasma radius. Using this expression for the case when the plasma radius is half the radius of the solenoid, we calculate the maximum displacement of the plasma boundary with respect to the beta value. The limit on the equilibrium beta comes from the fact that the plasma boundary is limited by the transverse dimension of the device. In Fig. 9 we show the displacement for three different solenoid radii. The larger solenoid radius leads to larger value of maximum equilibrium beta.

From Fig. 9 we note that our maximum equilibrium beta is ~ 5.5%. These numbers are only estimates and should be used only for order of magnitude estimates. In the theoretical treatment no mirror magnetic field is assumed

in the straight section. However, we may estimate that with a mirror ratio of 4, the maximum beta value in the straight section could be ~ 20%.

VII. Discussion of results

From the numerical and analytical results it is clear that the field lines and single particle orbits are well confined. This means that most of the passing particles do not diffuse outwards without a collision. Hence, the main purpose of carrying particles from one straight section into the next one seems to be well served by helical links.

Another very important result is the fact that the single-particle orbits do not depend upon pitch angle beyond a certain threshold value. It is possible to adjust the mirror ratio in the helical and straight sections, so that the pitch angle in the middle of helical and straight sections are already above the threshold value. Thus in a collisionless picture one would assume that there should be no pitch angle scattering in the helical section, thus reducing the outward diffusion to a large extent. However this picture would change somewhat in the presence of collisions as discussed in section 2.

It is interesting, at this point, to compare the properties of our scheme with those of the most popular magnetic confinement systems. The comparison can only be sketchy at best, so far, because our understanding of helically linked mirrors is still in a rudimentary stage. The confined particles can be divided into three classes: (1) particles trapped in the straight axisymmetric mirrors, (2) particles in the loss-cone of these mirrors (these are called "passing particles" in the nomenclature of toroidal confinement), and (3) particles trapped in the helical sections. Particles of the first class have

not been dealt with in this paper although in a real application of this scheme they would make up the bulk of the plasma. Their behavior is assumed to be standard and simple. In the absence of ballooning and drift instabilities, at least, their radial transport may be assumed to be slow compared to other loss rates. The particles in the third class, on the other hand, will be subject to consecutive drift excursions, i.e., their radial transport will be similar to that of trapped particles in stellarators or tokamaks.

Unfortunately, in the simple helical bends investigated here, we find that the particles trapped in the bends seem to get lost fast. We feel that this takes place because of the following scenario. Particles trapped in the helical section bounce back and forth in the section. As discussed earlier the particles tend to follow the field lines and the deviation from the field lines is due to the curvature and gradient-B drifts. The typical effect of curvature and gradient drift is to move the particles in the direction of the principal normal and this movement does not get affected by the direction of longitudinal motion. Thus a particle feels the drift in the same direction, regardless of whether it is going back or forth. On the other hand the rotational transform depends upon the direction of transit. Thus a particle going back and forth has the effect of rotational transform cancelled. Hence the net effect is that trapped particles keep moving outward until they get ripple trapped and eventually lost. However, there are two processes which decrease this loss. One is collisions, which may detrap the particle and the other is the ambipolar field, which provides some poloidal drift and reduces the loss to some extent [12]. Even then most of the particles which get trapped are lost to the device. However this loss is much lower than the ordinary mirror loss, as the density in the helical section would be

considerably lower than the straight sections. The effect of high loss of particles would always keep the density in the helical section low and thus the trapping rate due to collision would be less also. A very crude comparison of the ordinary mirror loss and the loss in our scheme can be made as follows. The loss depends on the density of particles in the helical section, the volume of the helical section and the fraction of passing particles subject to loss. We assume that the scattering rate in the long straight mirror sections is fast enough to keep the velocity distribution isotropic, i.e., to keep the loss-cones filled. The density n_s in these regions is therefore expected to be uniform in space, all the way to the mirror throats. In the helical sections, on the other hand, the densities n_h drop to much lower levels because only few trapped particles remain there at any given time, i.e. any mirror ratio $R_h \equiv B_t/B_h > 1$ makes the velocity in the helical region anisotopic, and <u>only</u> the loss-cones are nearly filled. In a first approximation we can estimate that $n_h \lesssim n_s B_h/B_t \equiv n_s/R_h$, which is based on the assumption that the passing particles remain on their flux tubes.

If we denote the rate of scattering of a particle near the loss-cone boundary into (or out of) the loss-cone in the straight section by ν_s^{lc}; i.e.

$$\nu_s^{lc} \equiv n_s \langle \sigma\ v \rangle_s^{lc} \tag{16}$$

Then the rate of trapping of such a particle in the helical sections can be estimated by the following expression:

$$\nu_h^{tr} = \nu_h^{lc} = n_h \langle \sigma\ v \rangle_h^{lc} \lesssim n_s \langle \sigma\ v \rangle_h^{lc}\ B_h/B_t \approx n_s \langle \sigma\ v \rangle_s^{lc}\ B_h^2/B_s B_t$$

$$= \nu_s^{lc}\ B_h^2/B_s R_h \tag{17}$$

The latter relations are based on the observation that the distributions of particle speeds in the two regions are similar and that the areas in velocity

space of the loss-cone boundaries are inversely proportioned to the mirror ratios, so that $\langle\sigma\ v\rangle_h^{lc}/B_h \approx \langle\sigma\ v\rangle_s^{lc}/B_s$. The relation is only approximate because the anisotropy in the helical sections, and particularly the counterstreaming character in velocity space must be expected to introduce an additional deviation.

The total rate of trapping in the helical sections, and hence the upper bound of net particle loss through the mirror throats of the straight sections can now be related directly to the ordinary mirror loss: we define the confinement gain factor

$$G \equiv \frac{n_s V_s \nu_s^{lc}}{n_h V_h \nu_h^{lc}} \gtrsim R_h \ \frac{L_s}{L_h} \cdot \frac{B_h}{B_s} \cdot \frac{v_s^{lc}}{v_h^{lc}} \approx R_h^2 \ L_s/L_h \tag{18}$$

where the magnetic flux in the straight and helical sections is assumed equal and related to the respective volumes V_s and V_h, and lengths L_s and L_h by the equality $B_s V_s/L_s = B_h V_h/L_h$, and relation (17) is used to eliminate the scattering rates. We see that with $R_h = 2$ and $L_s > 5\ L_h$ a sizable gain in confinement time is expected.

Some suggestions have been made regarding removing the mirrors in the straight section and making the field in the helical section high. Thus the helical sections themselves act as mirror throats and we would have no problem of the trapped particles in the helical section. However, one misses the point that in this way we are, in a sense, making all the particles trapped in the straight section also go through the helical section partly and thus they would be subject to the same loss as the trapped particles in our device. The transit time between the mirroring point increases, but considerably larger fraction of the particles are involved in the process in this case. In our

opinion we would not be gaining anything, but may loose, in this way of linking.

Since they constitute only a small fraction of the total content of the device, it is conceivable that the net confinement could be better than that in purely toroidal devices that are otherwise equivalent. The average value of β that can be contained is not yet known because the stability limits must still be ascertained. The particles of most interest in the present context are the passing particles, and the study reported here therefore focuses primarily on this class. We have seen that particles with substantial velocity ratio $v_{\parallel}/v_{\perp} \equiv \gamma_v$ have well behaved orbits in the helical sections. We can assure adeque values of γ_v for particles passing through the bends by making the ratio B_t/B_h sufficiently large. The disadvantage of the latter is that particles can and will become deeply trapped in the helical sections so that they loose all chances of getting detrapped before they are lost radially. We thus end up with the following picture. We make the straight sections much longer than the helical sections so that the total rate of transition between trapped and passing particles in the former is much larger than in the latter. We can therefore assume that the loss-cone in the straight mirror remains filled, the distribution in velocity space stays almost isotropic there. The same is not the case in the helical sections. Here the radial diffusion is fast enough so that the detrapping rate cannot balance the trapping rate. The net particle loss from the entire system is therefore dominated by the net trapping rate into the helical sections.

This situation needs to be compared with the tandem mirror arrangement. The complexity in construction of linked mirrors may be comparable or worse than that of tandem mirror arrangements. But there is a distinct advantage in

not requiring carefully maintained velocity distributions for thermal barriers and ambipolar potential control. More important, however, is the realization that electrostatic potential plugs in tandem mirrors contain low energy particles much better than high-energy particles which can escape out the ends if their energy exceeds the barrier height. The opposite is true for our linked mirrors where the trapping rate, and hence the loss rate, in the helical sections is much lower for energetic particles than for the low-energy component.

A serious problem of linked mirrors, in addition to the stability question, is the large size that such systems are likely to have. This problem is also mentioned by the proponents of the Dracon device [3]. The latter has considerable similarity with ours, but the links are more complex and do not provide a rotational transform.

VIII. Conclusion

The good confinement of passing particles in the device means that helical linking does the important job of transporting particles from one straight section to the next one very well. This implies substantial recovery of the particles, which would have been lost otherwise. We may expect a reasonably high value of beta in the straight section. However the problem of stability of the device needs to be solved. Use of noncircular coils is being studied. Stabilization using ponderomotive forces is also possible.

Concluding, we would say that steady state operation of the device along with reasonably high value of average beta and without the problem of longitudinal loss, make the scheme of helical linking of mirrors an attractive proposition which deserves to be pursued further.

Acknowledgements

We would like to thank N.E. Abt for providing us with the source of the codes he developed during the initial investigation of this device. We would also like to thank Alicia Ehrhardt (PPPL) for making available the source of the 'HELIAC' code.

References

[1] Logan, B. G., et al., "Mirror Advanced Reactor Study", UCRL-53333 (1983).

[2] Cordey, J. G. and Watson, C. J. H., in Proc. 5th European Conference on Controlled Fusion and Plasma Physics, Grenoble (1972) 98.

[3] Glagolev, V. M., Kadomtsev, B. B., Shafranov, V. D. and Trubnikov, B. A., in Controlled Fusion and Plasma Phys. (Proc. 10th European Conference, Moscow, 1981, Vo. 1, E-8.

[4] Hedrick et al., in Plasma Physics and Controlled Fusion Research 1984 (Proc. 10th Int. Conf. London 1984), IAEA, Vienna (1985) 630.

[5] Kunkel, W. B., Bull. Am. Phys. Soc. 27, 936 (1982).

[6] Abt, N. E. and Kunkel, W. B., Bull. Am. Phys. Soc. 28, 1033 (1983).

[7] Leontovich, M. A., (Ed.), in Reviews of Plasma Physics, Vol. 5, Consultants Bureau, New York (1966) 45.

[8] Leontovich, M. A., (Ed.), in Reviews of Plasma Physics, Vol. 5, Consultants Bureau, New York (1966) 207.

[9] Ehrhardt, A., Princeton Plasma Physics Laboratory (1985). (Private Communication)

[10] Foote, J., "TIBRO-X: a code to compute trajectories of charged particles in magnetic fields", UCRL-52189 (1976).

[11] Leontovich, M. A., (Ed.), in Reviews of Plasma Physics, Vol. 5, Consultants Bureau, New York (1966) 135.

[12] Hitchon, W. N. G., et al., J. Plasma Physics (1985), vol. 34, part 2, 327.

Figure Captions

Fig. 1 A view of THELMA, with generating cylinder inserted. Note that circular loops have been represented as polygons. "H", "S", and "G" represent helical section, straight section and generating cylinder respectively.

Fig. 2. Schematic representation of magnetic field on and off-magnetic axis (not to scale). Solid and dashed lines represent field on-axis and off-axis respectively. B_s, B_t and B_h represent field in the straight section, throat and helical section respectively.

Fig. 3. Expected magnetic surface in the middle of helical section on the basis of theoretical model. Principal normal is towards the right side. Notice the crowding of surfaces in that direction.

Fig. 4. Computed magnitude of B along the magnetic axis for (a)case with no mirror and (b) case with mirrors in the straight section. Notice the three-fold symmetry. The data used is for the actual coil system studied. The zero of the azimuthal angle is in the middle of a helical section.

Fig. 5. Puncture plot (a) in the middle of straight section and (b) in the middle of helical section. Different symbols represent different surfaces. Notice that they seem to form distinct closed magnetic surfaces. The larger symbol represent starting point and the medium sized symbols the point after one complete round of device.

Fig. 6. Rotational transform in degrees vs. radial distance (ra). Note that rotational transform has been computed for one turn of field lines only.

Fig. 7. Radial distance of drift orbit vs. distance along geometric axis. Notice that the radial distance from the axis remains nearly constant in the straight section, but changes in the helical section.

Fig. 8. Drift orbit puncture plot in the middle of the helical section and its variation with (a) radial distance, (b) pitch angle ($v_{\parallel}/v_{\perp}$ = 2.0,5.0, 50.0); note that all of them are indistinguishable, as expected theoretically, (c) sign of charge. An ellipse has been fitted to the puncture points.

Fig. 9. (Maximum displacement of plasma column/radius of solenoid) vs. beta for solenoid radius, a=0.08, 0.10 and 0.125 m.

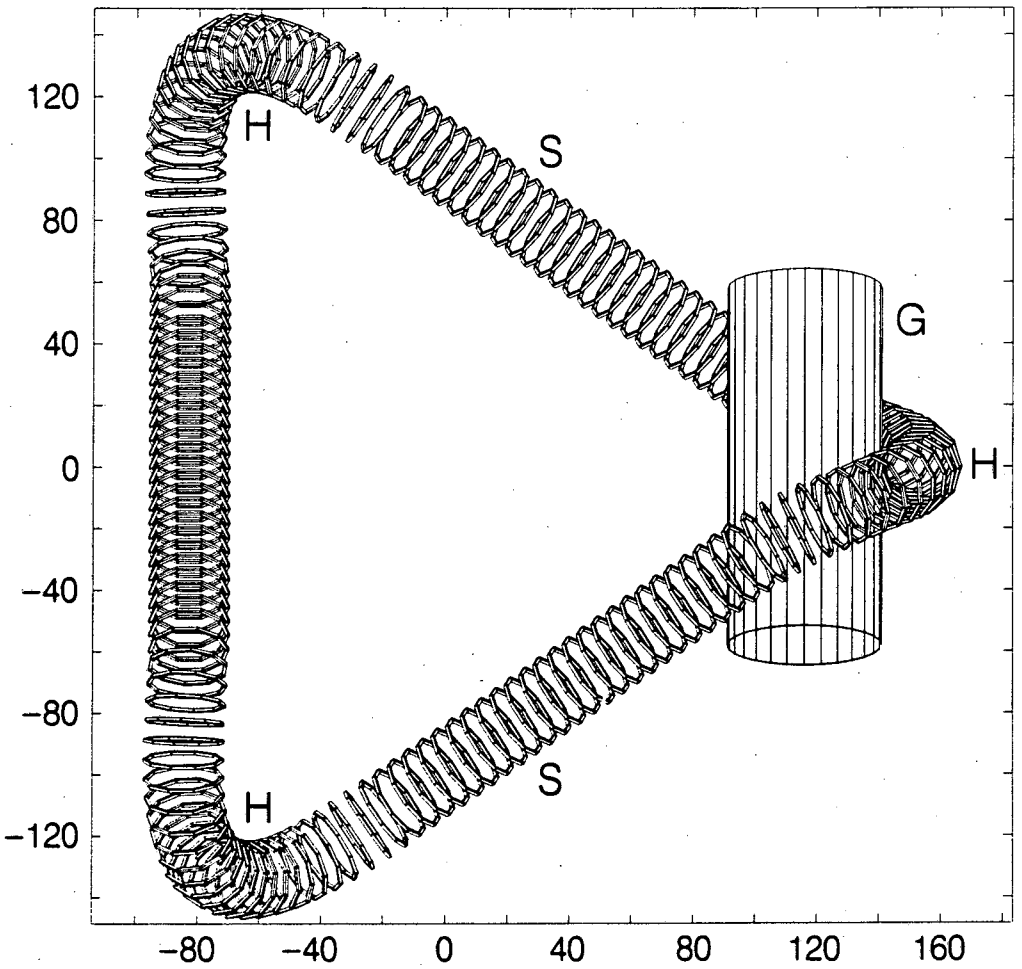

XBL 862-9744

Fig. 1

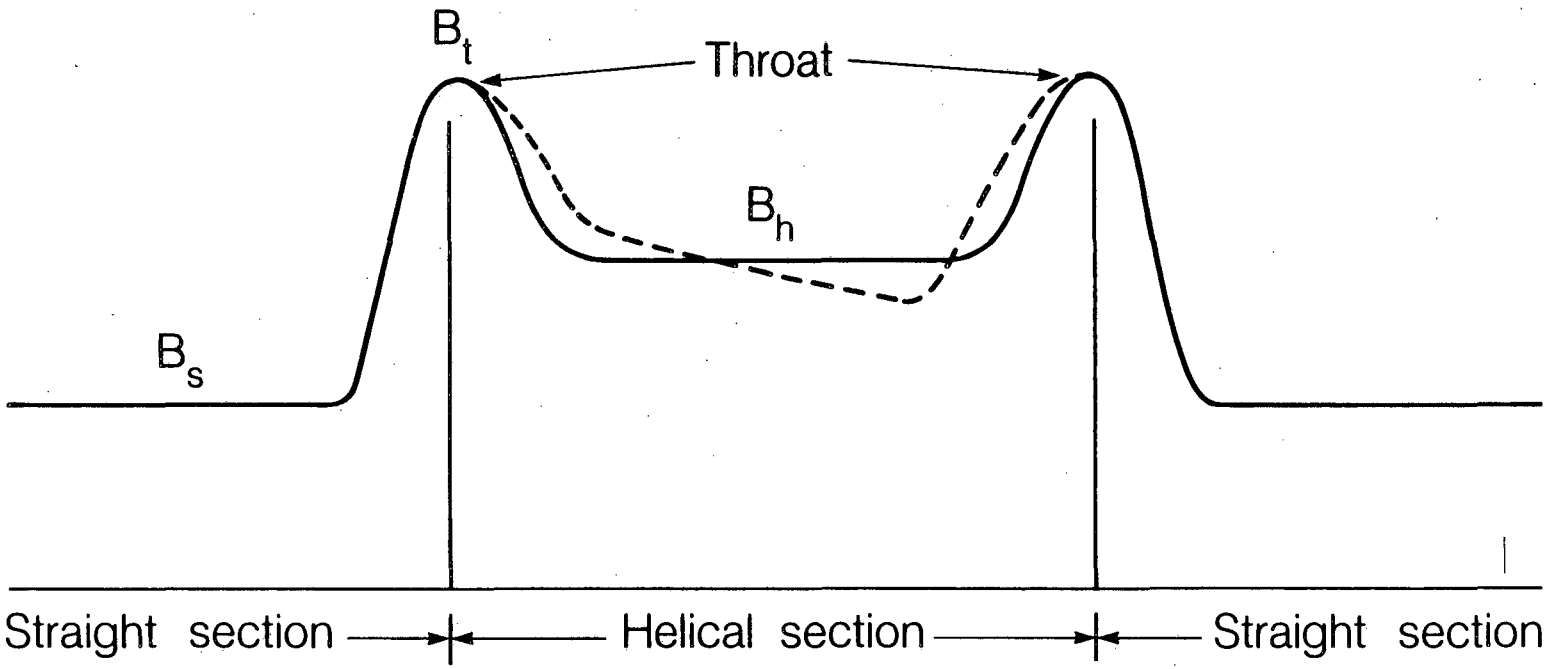

XBL 862-9735

Fig. 2

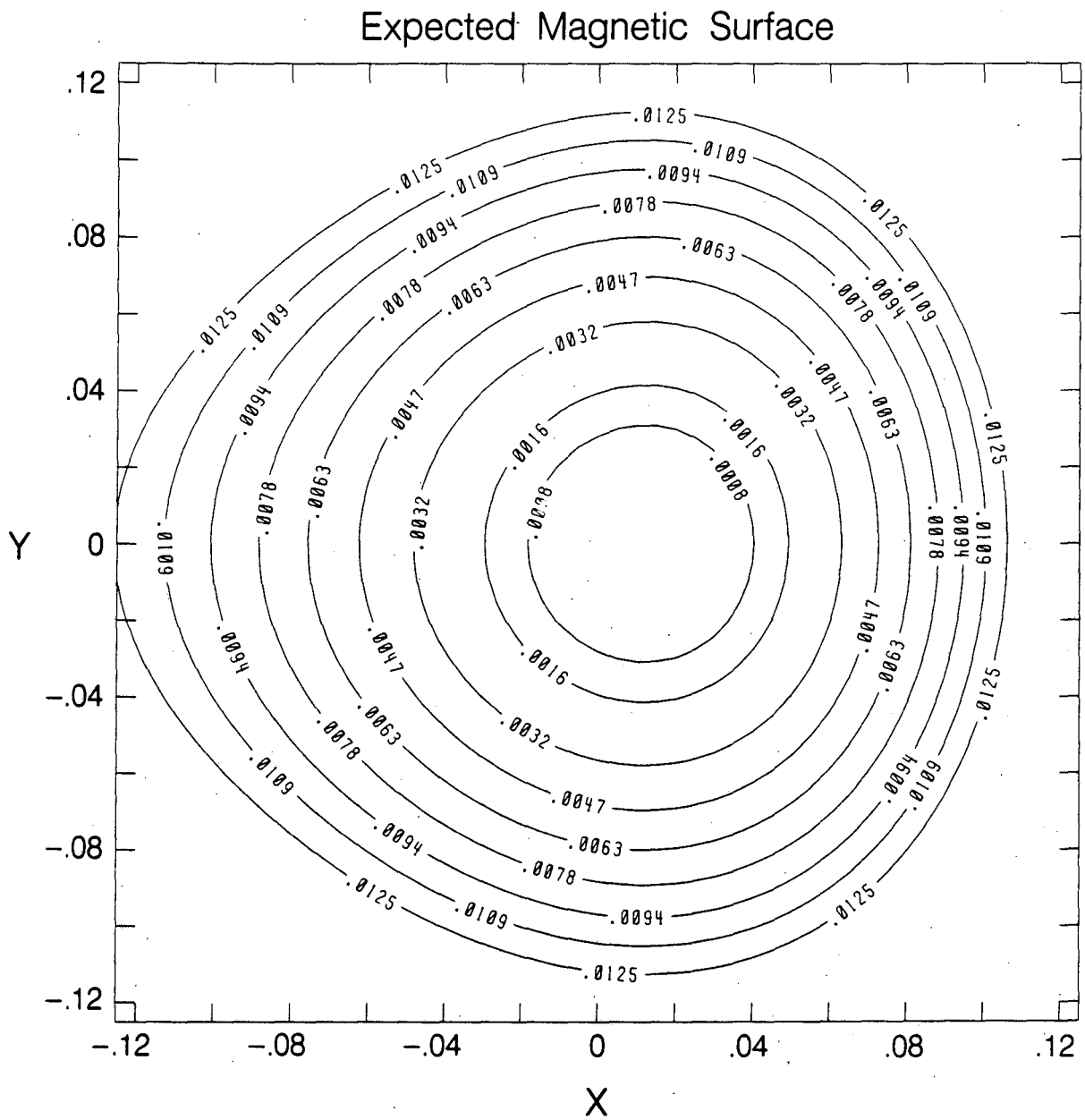

XBL 862-9746

Fig. 3

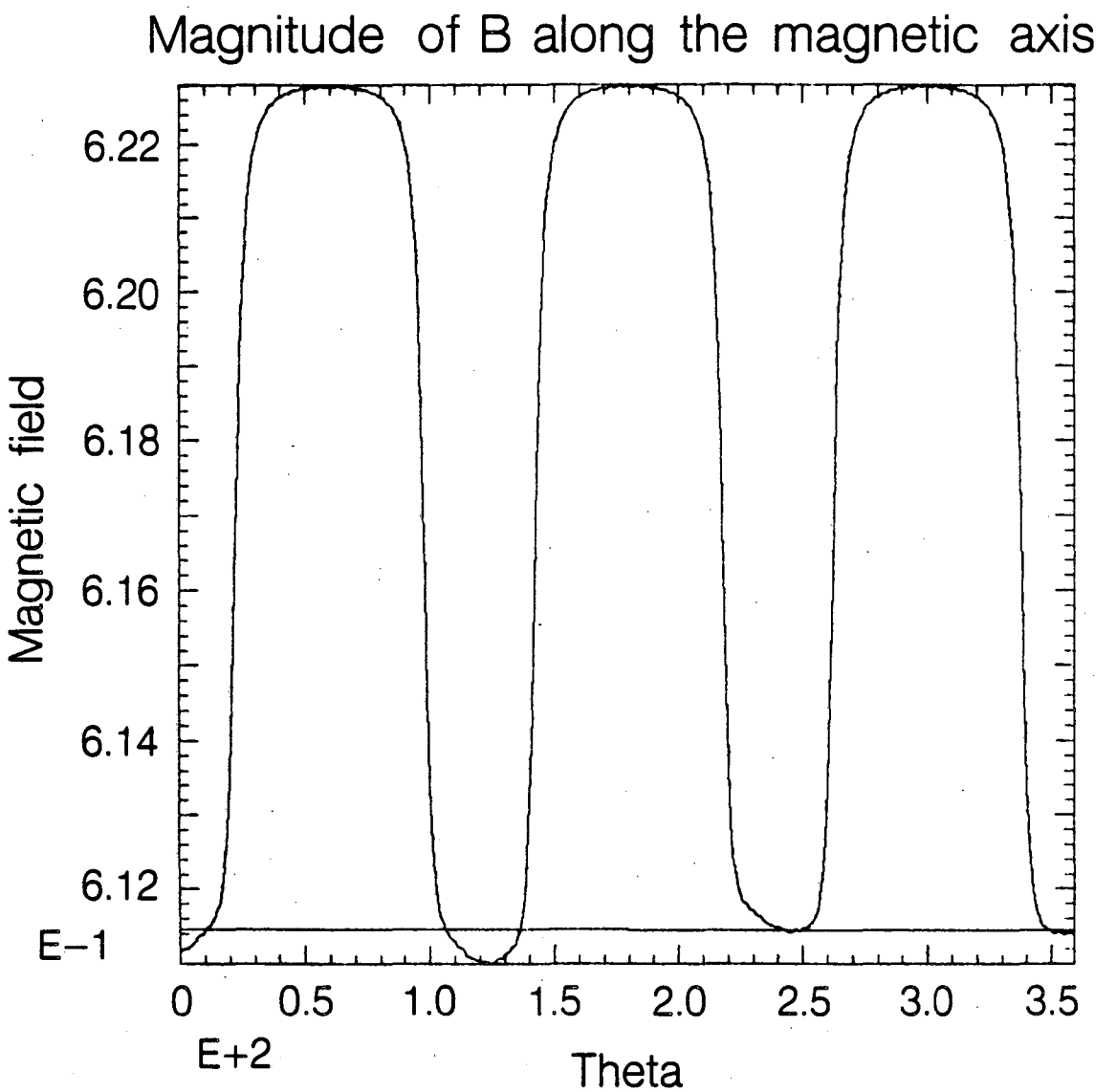

XBL 862-9737

Fig. 4a

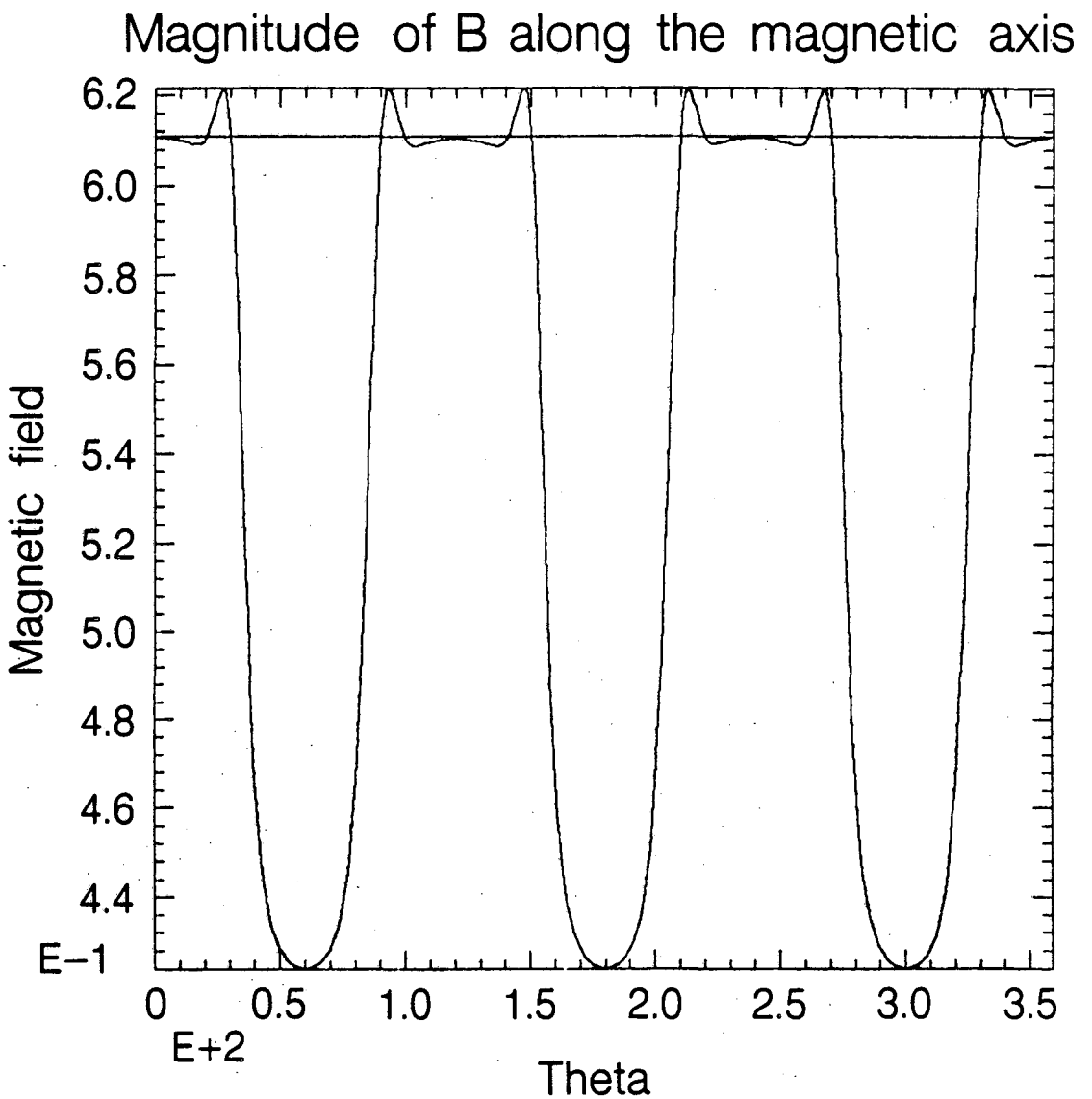

XBL 862-9738

Fig. 4b

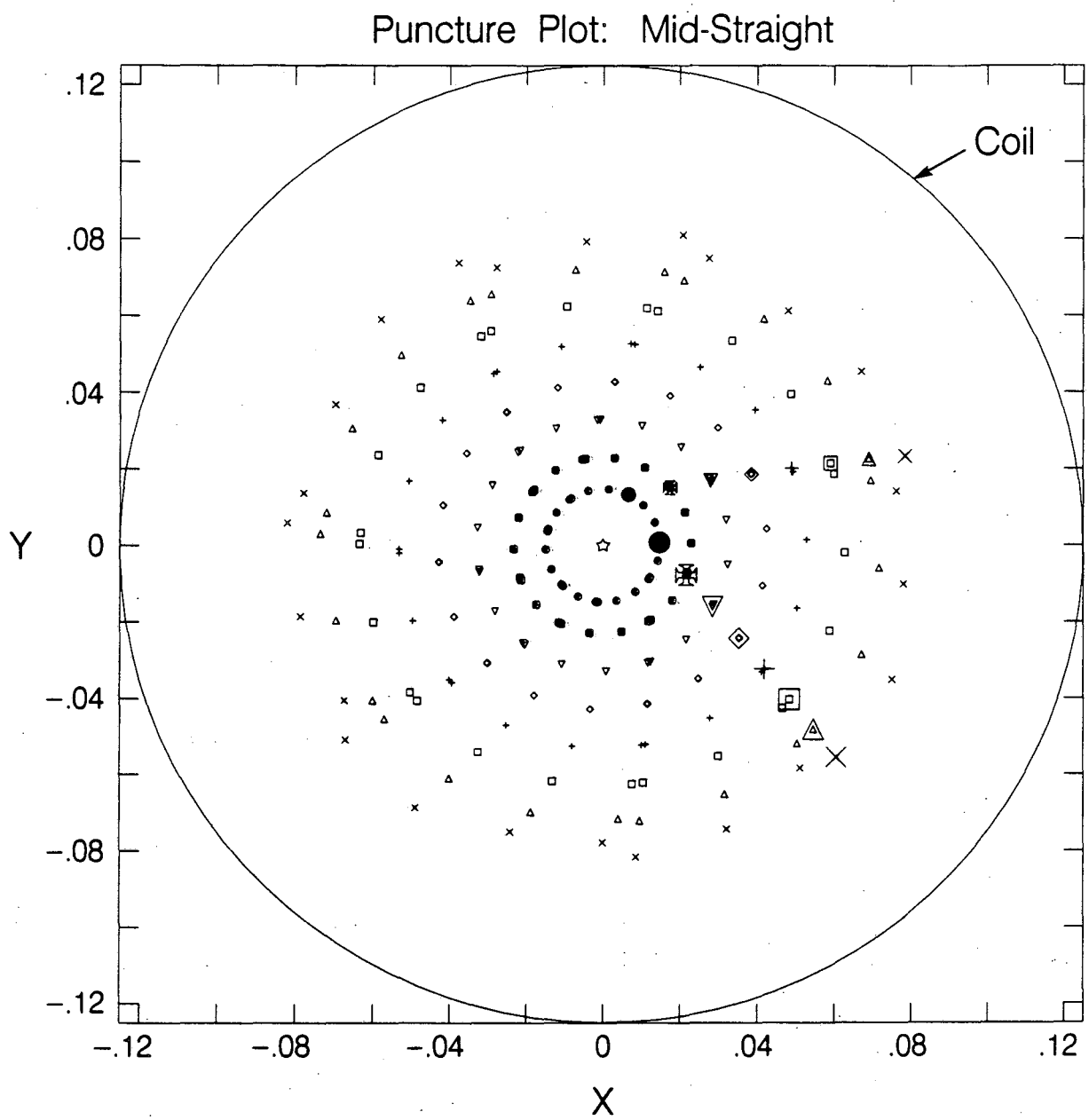

XBL 862-9747

Fig. 5a

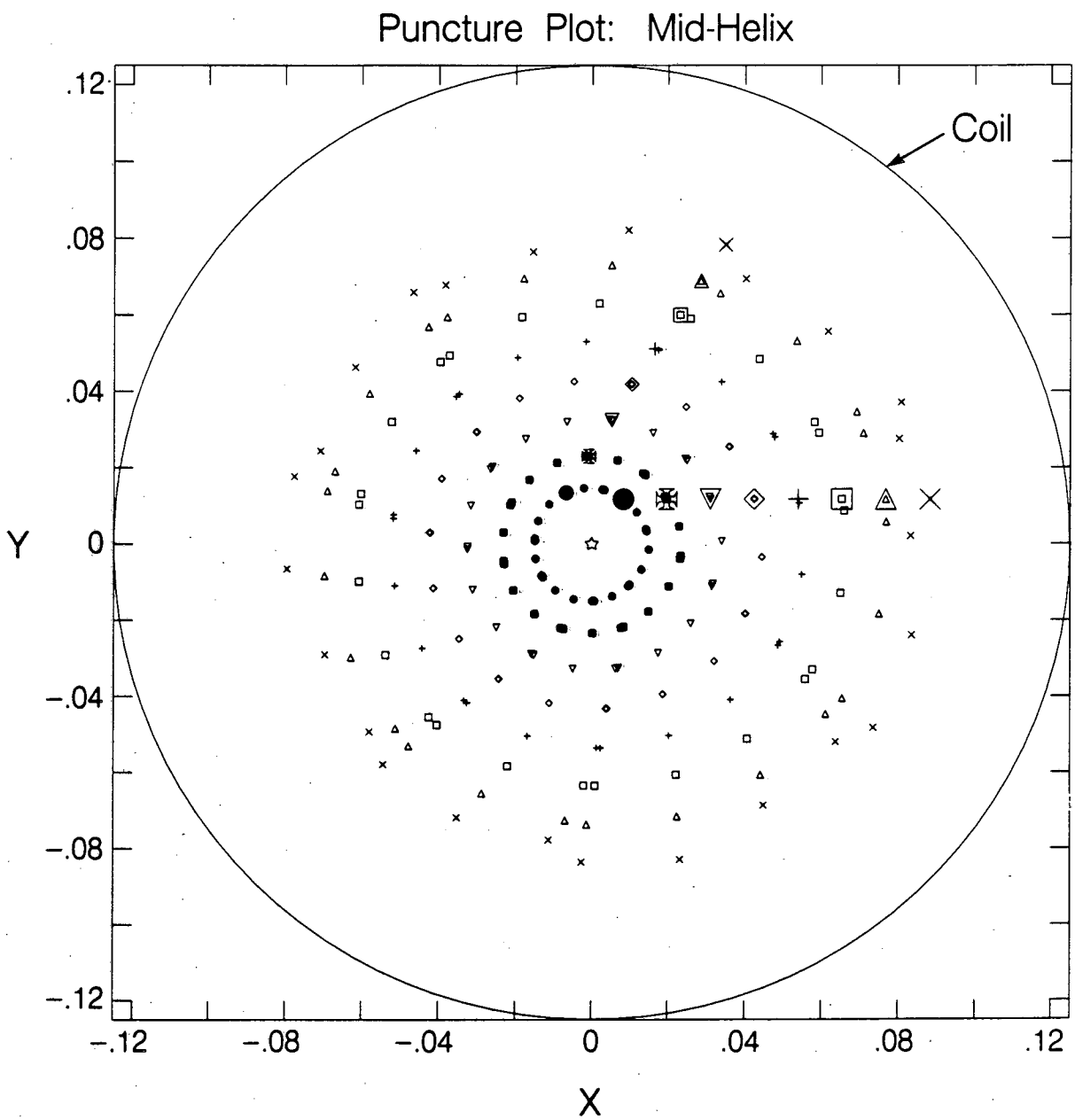

XBL 862-9745

Fig. 5b

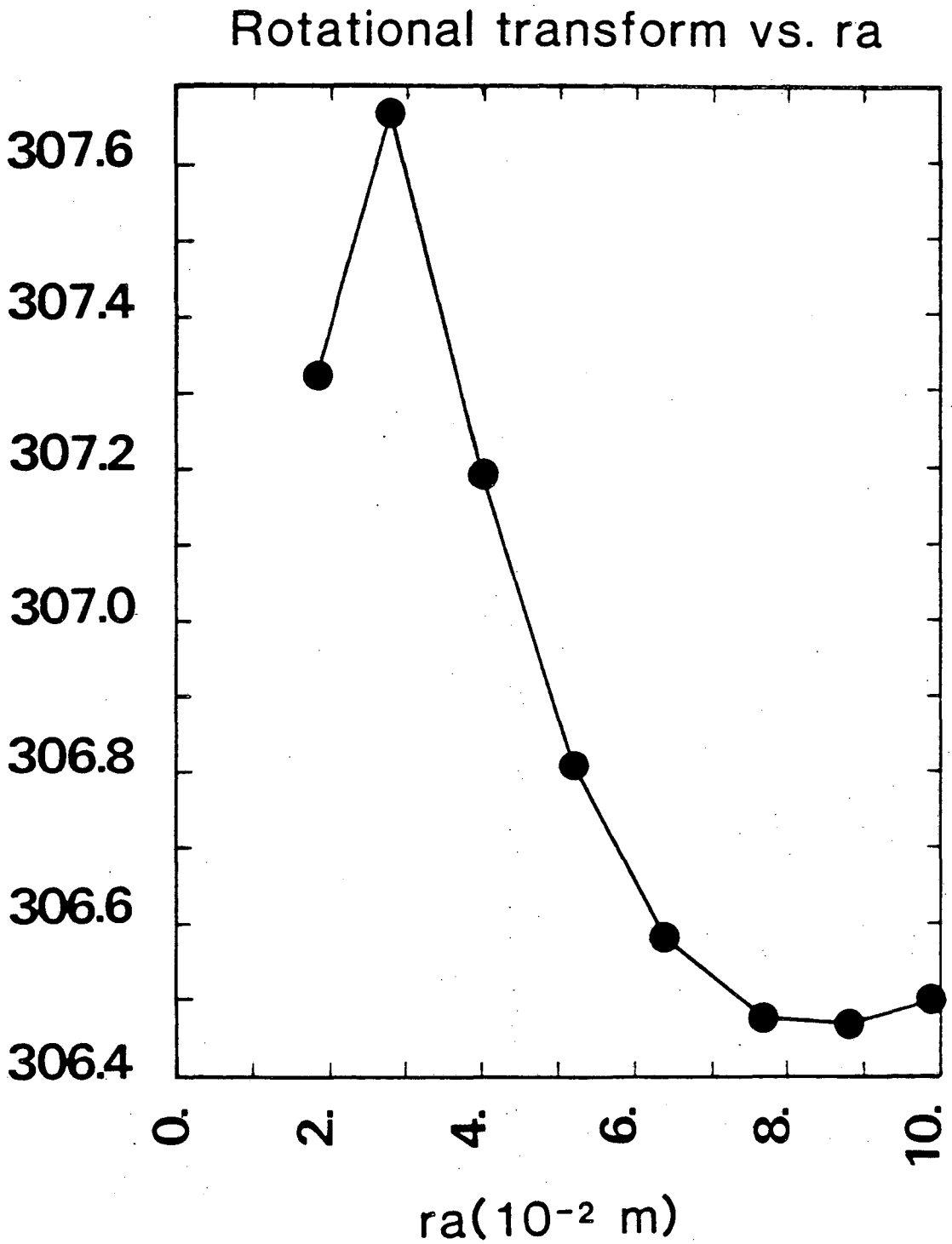

XBL 862-9739

Fig. 6

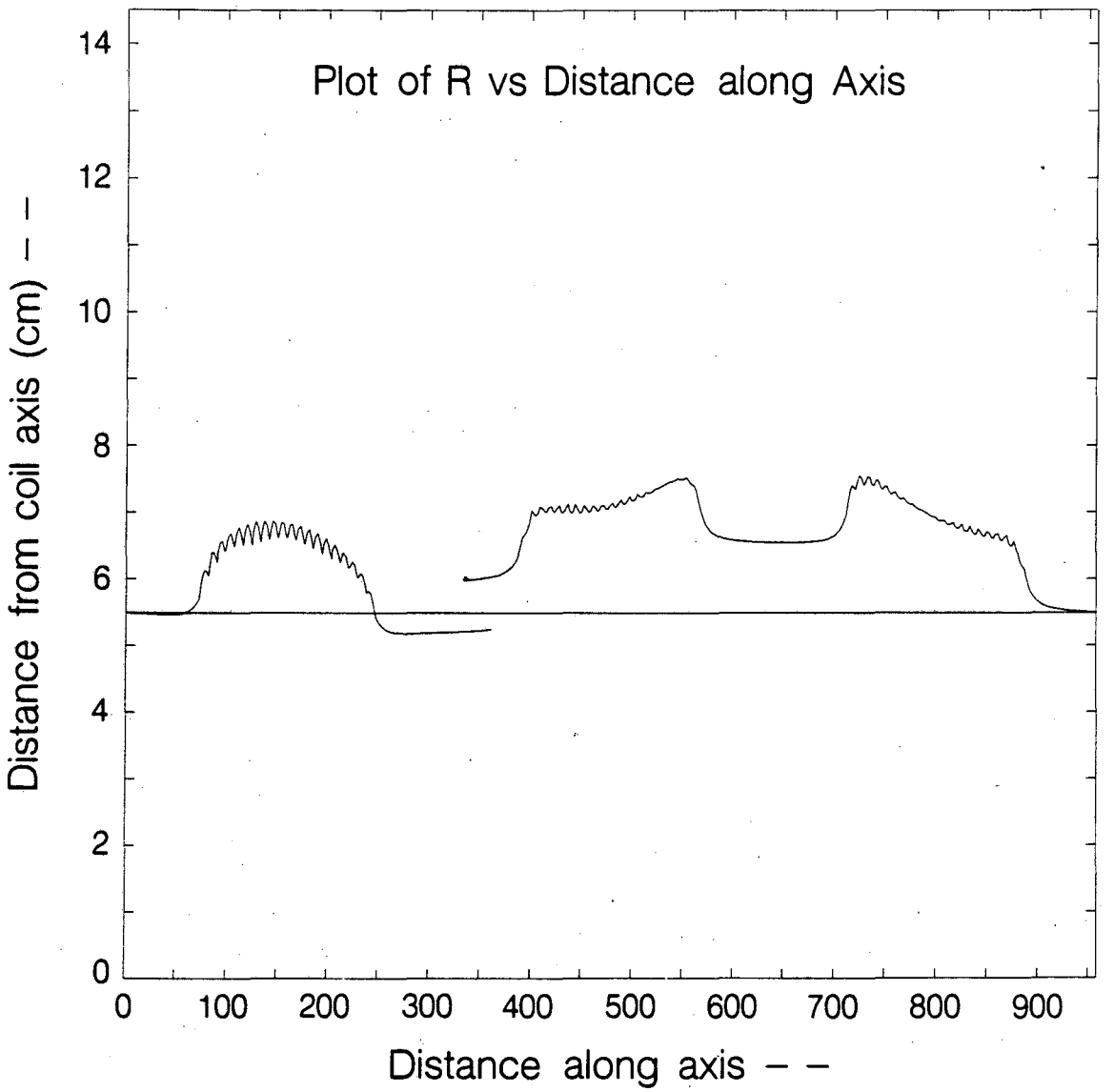

XBL 862-9740

Fig. 7

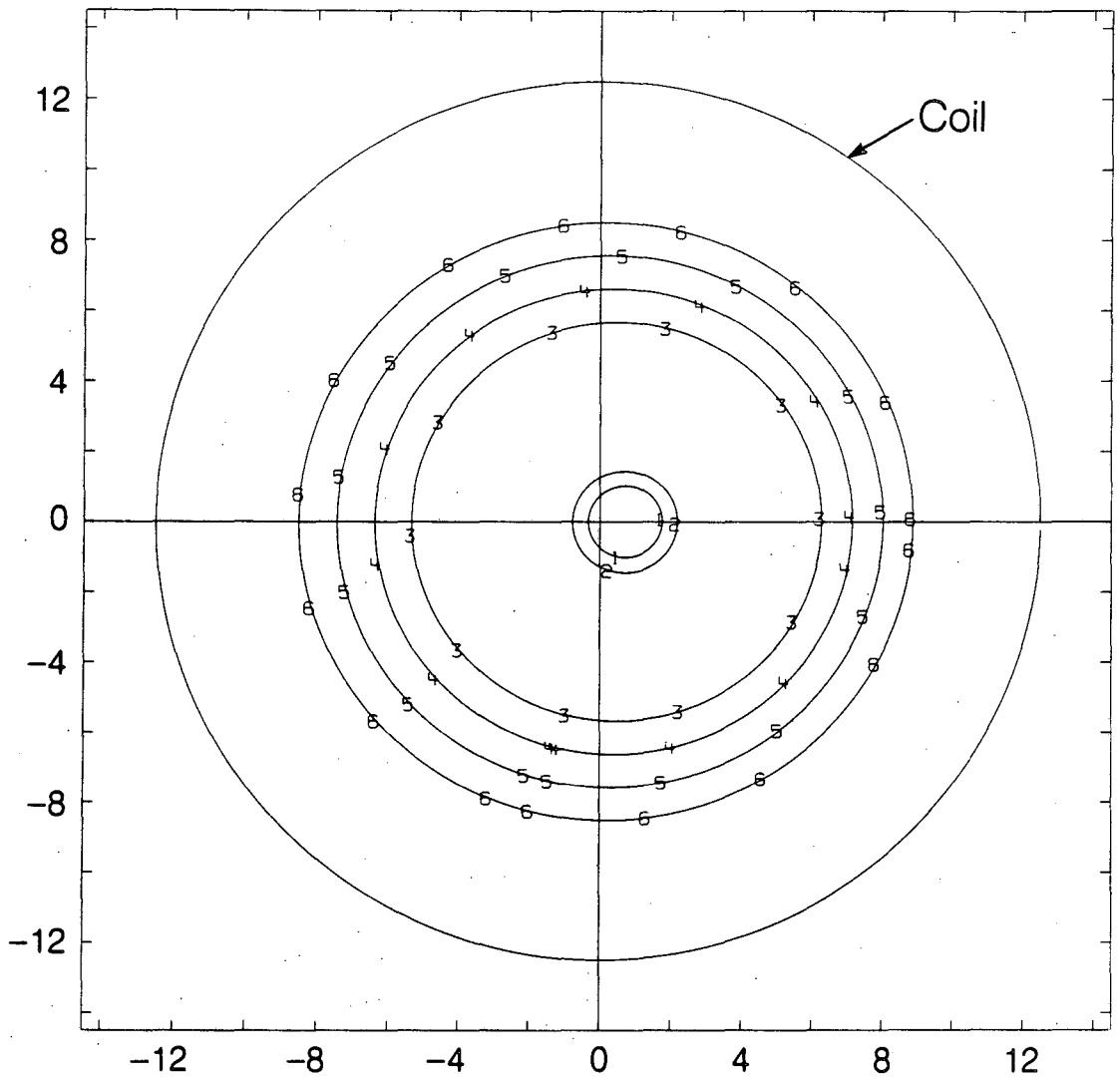

XBL 862-9741

Fig. 8a

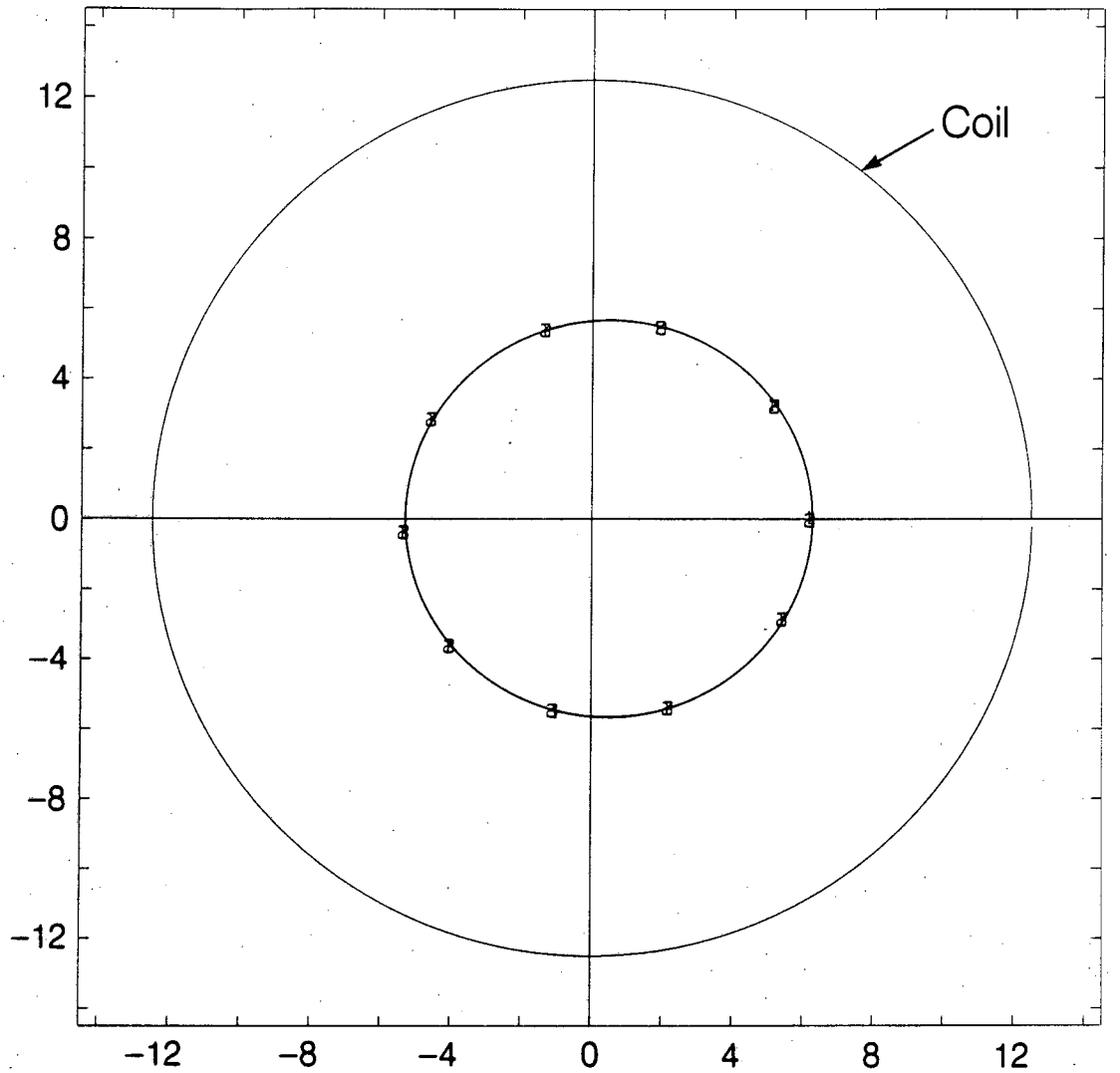

XBL 862-9743

Fig. 8b

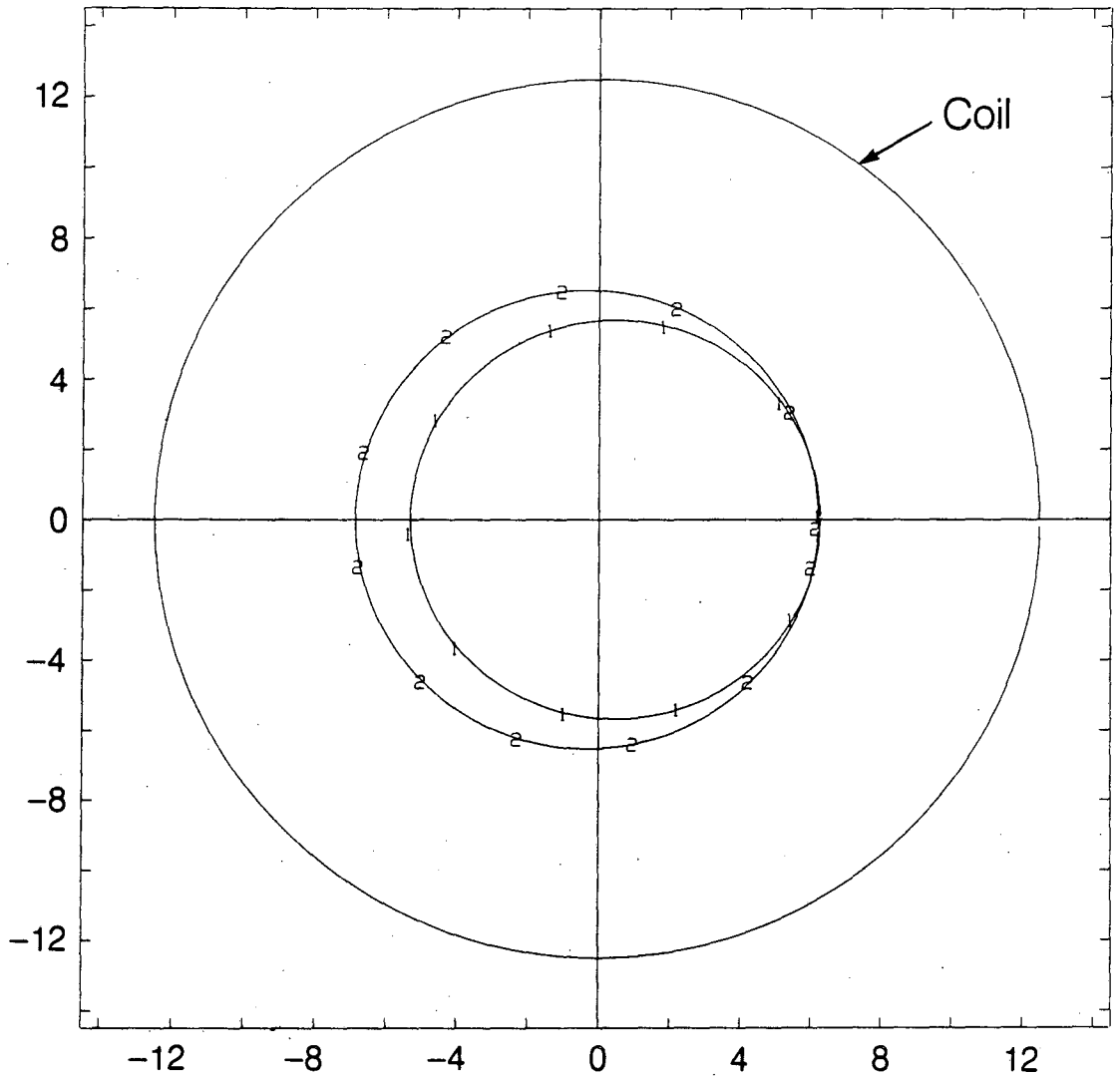

XBL 862-9742

Fig. 8c

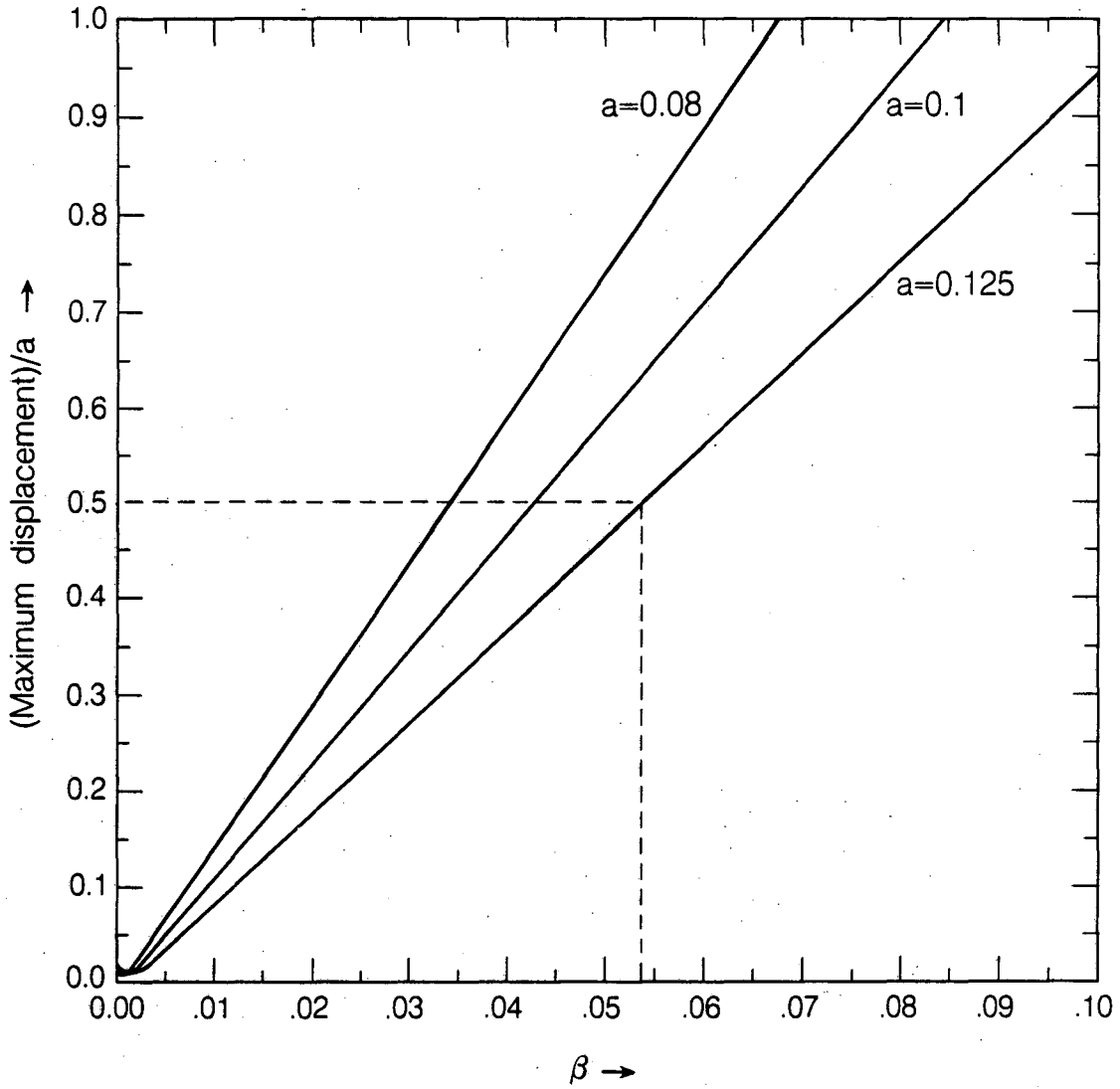

XBL 862-9736

Fig. 9

This report was done with support from the Department of Energy. Any conclusions or opinions expressed in this report represent solely those of the author(s) and not necessarily those of The Regents of the University of California, the Lawrence Berkeley Laboratory or the Department of Energy.

Reference to a company or product name does not imply approval or recommendation of the product by the University of California or the U.S. Department of Energy to the exclusion of others that may be suitable.

LAWRENCE BERKELEY LABORATORY
TECHNICAL INFORMATION DEPARTMENT
UNIVERSITY OF CALIFORNIA
BERKELEY, CALIFORNIA 94720